



Prediction of Ferrite Number of Duplex Stainless Steel Clad Metals Using RSM

Response surface methodology (RSM) was used to establish a relationship between process parameters and Ferrite Number for duplex stainless steel clad metals

BY T. KANNAN AND N. MURUGAN

ABSTRACT. Duplex stainless steel clad metals contain delta ferrite, which is expressed in terms of Ferrite Number (FN). The amount of ferrite present in the deposit is a function of chemical composition of the filler and base metals, welding process, type of shielding gas, welding procedure, and heat input during cladding. Excessive ferrite in duplex stainless steel claddings can result in poor ductility, toughness, and corrosion resistance. Likewise, insufficient ferrite can also produce inferior mechanical and corrosion resistance properties. Hence, control of ferrite in duplex stainless steel cladding is essential to obtain the required mechanical and corrosion-resistant properties.

This paper highlights the application of response surface methodology to develop mathematical models and to analyze various effects of flux cored arc welding (FCAW) process parameters on the FN of duplex stainless steel clad metals. The experiments were conducted based on four-factor, five-level, central composite rotatable design with full replications technique and mathematical models developed using multiple regression technique. The developed mathematical models are very useful for predicting and controlling the FN in duplex stainless steel cladding. The main and interaction effects of input process parameters on calculated FN (by WRC-1992 diagram) and measured FN have been presented in graphic form, which helps in selecting FCAW

process parameters to achieve the required FN.

Introduction

Weld cladding is a process in which a thick layer of a weld metal is deposited onto a carbon- or low-alloy-steel base metal to provide a corrosion-resistant surface. It finds extensive use in numerous industries such as paper, chemical, fertilizer, nuclear, food processing, petrochemical, and other allied industries. The desirable characteristics of cladding material are reasonable strength, weldability to the steel, resistance to general and localized corrosion attack, and good corrosion fatigue properties (Ref. 1). In recent years, duplex stainless steel is extensively used for weld cladding because it has excellent chloride stress corrosion cracking resistance, pitting and crevice corrosion resistance, yield strength, ductility, impact toughness, and weldability (Ref. 2).

The composition and properties of clad metals are strongly influenced by dilution, as illustrated in Fig.1. It is the amount of base metal melted (B) divided by the sum of the filler metal added and base metal melted (A+B). Dilution re-

duces the alloying elements and increases the carbon content in the clad layer, which reduces corrosion resistance properties and causes other metallurgical problems. It also affects the ferrite content in claddings. The amount of ferrite present in duplex stainless steel clad metals influences mechanical and corrosion properties. Both strength and stress corrosion cracking resistance may be reduced when the FN is less than 30, and there is a loss of both ductility and toughness of the clad metal when the FN is above 70 in duplex stainless steel weld claddings (Ref. 3). Hence, control of the FN is essential to achieve optimum corrosion resistance and mechanical properties (Ref. 4). This can be effectively done by properly selecting the process parameters after thoroughly understanding the direct and interaction effects of process parameters on dilution.

The economics of stainless steel weld cladding are dependent on achieving the specific chemistry at the highest practical deposition rate in a minimum number of layers (Ref. 5). Heat input also affects the FN. Ferrite Number increases with a decrease in heat input. With increasing cooling rate (low heat input), the solid-state transformation is suppressed, and the residual ferrite content increases.

In stainless steel weld cladding, it is essential to understand how the dilution affects the composition and FN so as to control the corrosion resistance and mechanical properties.

During the last two decades, four constitution diagrams have found the widest application in predicting ferrite content from weld deposit composition. These include the Schaeffler Diagram, DeLong Diagram, WRC-1988 Diagram, and WRC-1992 Diagram. The Schaeffler Diagram, published in 1947, has been exten-

KEYWORDS

Duplex Stainless Steel
FCAW
Ferrite Number
Heat Input
Mathematical Models
Response Surface
Methodology

T. KANNAN (kannan_kct@yahoo.com) is an assistant professor of mechanical engineering, Kumaraguru College of Technology, Coimbatore, Tamil Nadu, India. N. MURUGAN (drmurugan@yahoo.com) is professor of mechanical engineering, Coimbatore Institute of Technology, Coimbatore, Tamil Nadu, India.

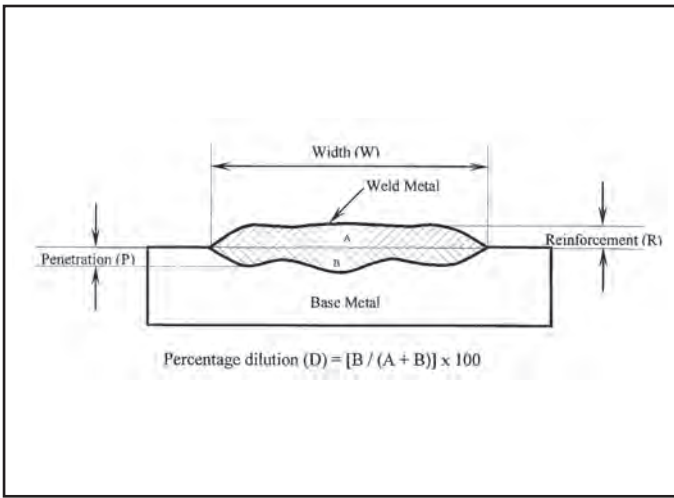


Fig. 1 — Weld bead geometry.

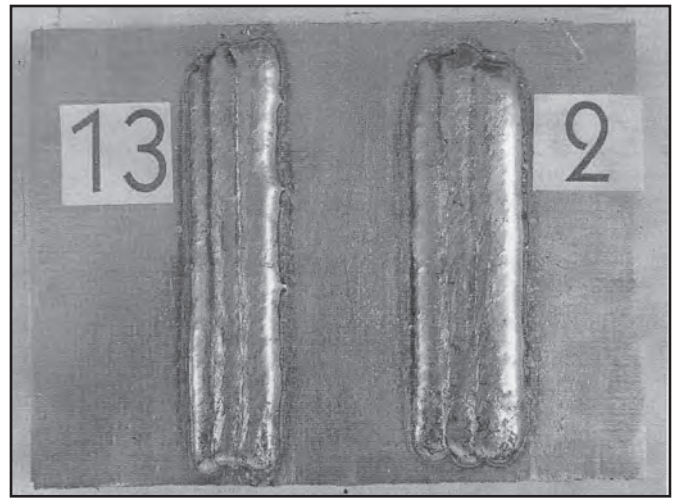


Fig. 2 — Typical clad plate (Trial Nos. 13 and 2).

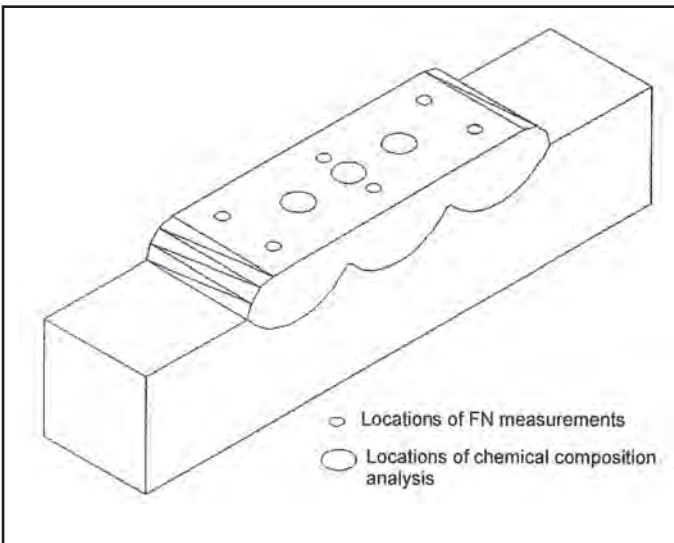


Fig. 3 — Locations of the FN and chemical analysis measurements.

sively used for estimating the ferrite content of stainless steel weld metals and weld microstructure from its composition (Ref. 6). This diagram does not consider the powerful effect of nitrogen in promoting austenite, which tends to seriously overes-

timate the weld metal ferrite (Ref. 7). Also, the Schaeffler Diagram was used to predict the ferrite in terms of “percent ferrite,” which is imprecise. The second widely used prediction diagram, the DeLong Diagram, was published in 1974 and incorporated some improvements (Ref. 8). It has a FN scale and includes a coefficient for nitrogen in the nickel equivalent. This diagram is specifically designed for 300-series stainless steel welds containing small amounts of ferrite.

Prediction of the FN in duplex stainless steel welds is not possible using the DeLong Diagram because nickel and chromium equivalents fall outside the range of this diagram (Ref. 4).

The WRC-1988 Diagram overcomes many of the problems associated with the Schaeffler and DeLong Diagrams (Ref. 4). It was developed with data measured by the most recent definition of the FN scale. In recent years, duplex stainless steels have been used more frequently. Some of these steels and their weld metals contain significant amounts of copper, which is not included in nickel equivalent of WRC-1988 Diagram, and hence, its FN prediction accuracy is less.

The WRC-1992 Diagram (Ref. 9) is the most recent of the diagrams mentioned above, and it is officially adopted by the ASME Boiler and Pressure Vessel Code for predicting the FN when the FN cannot be measured.

Among the four constitution diagrams used for estimating the FN of duplex stainless steel weld/clad metals from its composition, the WRC-1992 Diagram is more suitable due to the reasons below.

- It has a Ferrite Number (FN) scale.
- It includes a coefficient for nitrogen in the nickel equivalent.
- Nickel and chromium equivalents fall inside the range of this diagram.
- Copper term is included in nickel equivalent, hence, FN prediction accuracy is improved.
- Axes of the diagram can be extended to predict dilution effects in dissimilar

Table 1 — Chemical Composition of Filler and Base Metals

Material	Elements, %											FN
	C	Si	Mn	P	S	Al	Cr	Mo	Ni	N ₂	Cu	
IS: 2062	0.150	0.160	0.870	0.015	0.016	0.031	—	—	—	—	—	—
E2209T1-4/1	0.023	0.760	1.030	0.024	0.002	—	23.14	3.05	9.22	0.13	0.09	47

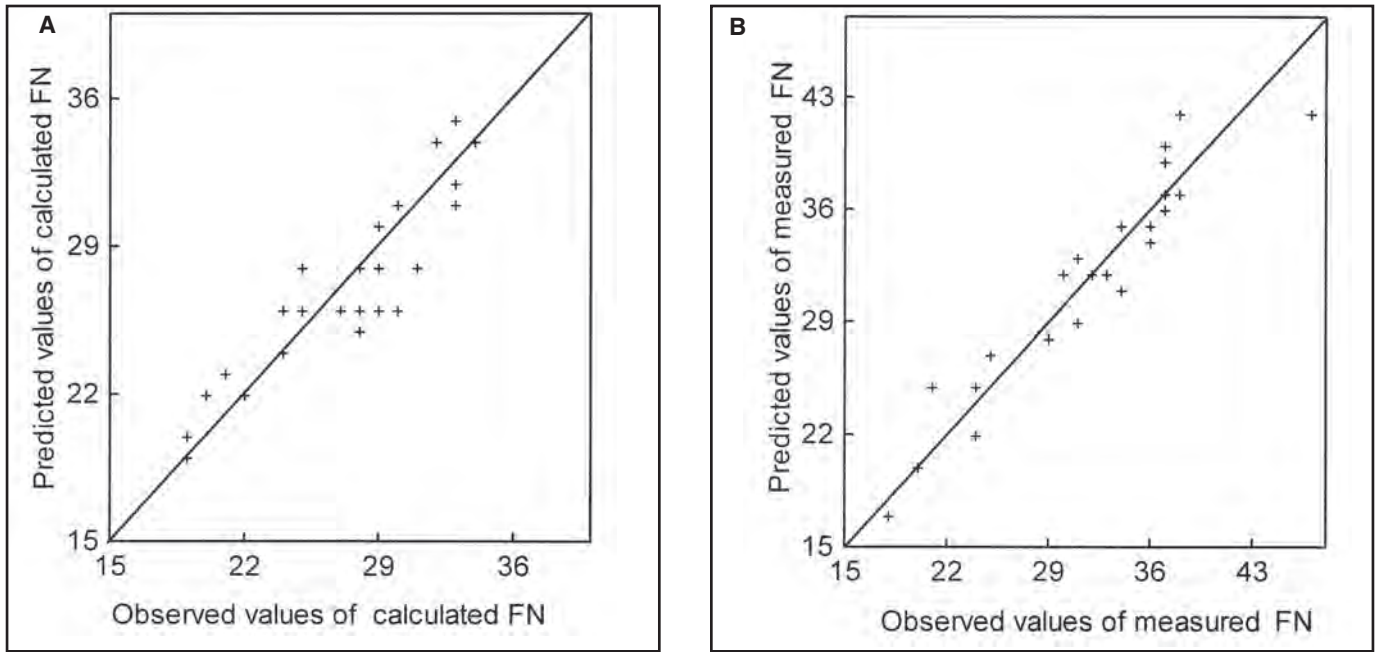


Fig. 4 — A — Scatter diagram of calculated FN model; B — scatter diagram of measured FN model.

Table 2 — Welding Parameters and Their Levels

Parameter	Unit	Notation	Factor levels				
			-2	-1	0	+1	+2
Welding current	A	I	200	225	250	275	300
Welding speed	cm/min	S	20	30	40	50	60
Contact tip-to-workpiece distance	mm	N	22	24	26	28	30
Welding gun (push) angle	degree	T	70	75	80	85	90

welding/cladding applications.

The above diagrams do not accurately reflect the effects of welding process, technique, and cooling rate on the FN. Therefore, a study on the effects of welding parameters on the calculated FN (by WRC-1992 Diagram) and the measured FN of duplex stainless steel clad metals may be useful. However, there is little published information available with regard to the effect of welding parameters on the FN of duplex stainless steel clad metals.

This paper highlights an experimental study carried out to analyze the effects of various FCAW process parameters on the calculated FN (by WRC-1992 Diagram) and the measured FN of duplex stainless steel cladding.

Experimental Procedure

The experiments were conducted using

a constant voltage programmable welding machine (UNIMACRO 501C). In this machine, welding current can be set directly instead of changing wire feed rate for changing current level. Test plates of size 200 x 150 x 20 mm were cut from low-carbon structural steel (IS: 2062) plate, and its surfaces were ground to remove oxide scale and dirt before cladding. Flux cored duplex stainless steel welding wire of 1.2 mm diameter was used for depositing the weld beads. The chemical composition of filler and base metals is given in Table 1. Carbon dioxide (CO₂) gas at a constant flow rate of 18 L/min was used for shielding. The experimental setup used consisted of a traveling carriage with a table for supporting the specimens. The welding gun was held stationary in a frame mounted above the worktable, and it was provided with an attachment for both up and down movement and angular movement for setting the required contact tip-

to-workpiece distance and welding gun angle, respectively. The experiments were conducted by laying three beads using a stringer bead technique with a constant overlap of 40%. An interpass temperature of 150°C was maintained during the cladding experiments.

Among the many independently controllable primary and secondary process parameters affecting the FN, the primary process parameters *viz* welding current (I) and welding speed (S), and the secondary process parameters *viz* contact tip-to-workpiece distance (N) and welding gun angle (T), were selected as process parameters for this study. The welding current, welding speed, and voltage are the primary parameters contributing to the heat input, influencing FN variations in the claddings. The machine used for this study was constant voltage type, hence it was decided to select the welding current and welding speed as primary process parameters. So far, few studies have been carried out on the effects of contact tip-to-workpiece distance and welding gun angle on the FN, therefore it was decided to select the contact tip-to-workpiece distance and welding gun angle (push angle) as secondary process parameters. The working ranges of all selected parameters were fixed by conducting trial runs. This was carried out by varying one of the factors while keeping the rest of them at constant values (Ref. 10). The working range of each process parameter was decided upon by inspecting the bead for a smooth appearance without any visible defects such as surface porosity, undercut, etc. The

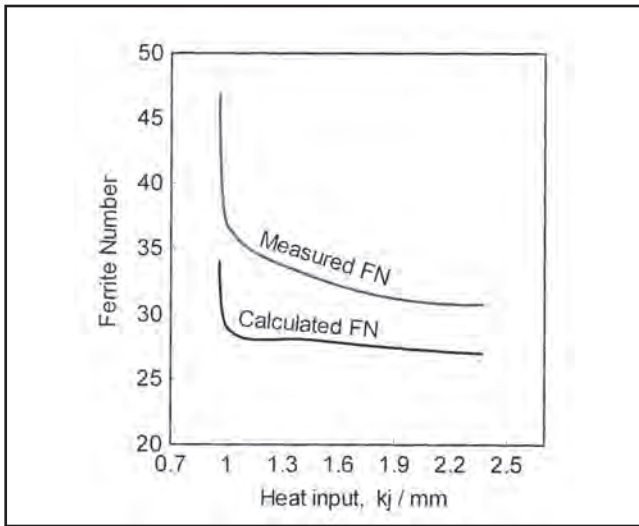


Fig. 5 — Effect of heat input on FN.

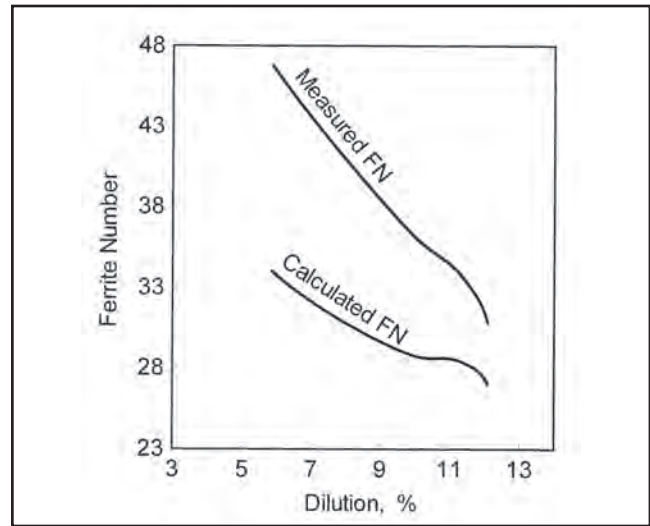


Fig. 6 — Effect of dilution on FN.

Table 3 — Design Matrix with FN and Dilution

Trial No.	Design matrix				Calculated FN (by WRC-1992)	Measured FN	Dilution (%)
	I	S	N	T			
01	-1	-1	-1	-1	33	37	07.86
02	+1	-1	-1	-1	27	31	12.10
03	-1	+1	-1	-1	31	36	11.35
04	+1	+1	-1	-1	22	24	11.98
05	-1	-1	+1	-1	33	38	06.54
06	+1	-1	+1	-1	28	34	08.82
07	-1	+1	+1	-1	29	37	09.69
08	+1	+1	+1	-1	24	25	11.16
09	-1	-1	-1	+1	30	38	08.97
10	+1	-1	-1	+1	29	31	13.75
11	-1	+1	-1	+1	21	21	18.52
12	+1	+1	-1	+1	19	20	20.58
13	-1	-1	+1	+1	32	37	07.46
14	+1	-1	+1	+1	29	34	09.14
15	-1	+1	+1	+1	28	25	18.00
16	+1	+1	+1	+1	20	24	14.80
17	-2	0	0	0	34	47	05.86
18	+2	0	0	0	24	25	16.48
19	0	-2	0	0	33	36	05.31
20	0	+2	0	0	19	18	17.35
21	0	0	-2	0	24	33	11.71
22	0	0	+2	0	33	37	09.01
23	0	0	0	-2	25	34	10.54
24	0	0	0	+2	24	29	13.98
25	0	0	0	0	29	32	10.33
26	0	0	0	0	25	30	13.60
27	0	0	0	0	30	33	10.73
28	0	0	0	0	28	33	11.71
29	0	0	0	0	25	30	13.76
30	0	0	0	0	24	33	10.99
31	0	0	0	0	24	33	10.67

upper limit of a factor was coded as +2, and the lower limit was coded as -2. The coded values for intermediate values were calculated using the equation

$$X_i = 2[2X - (X_{max} + X_{min})] / (X_{max} - X_{min}) \quad (1)$$

Where X_i is the required coded value of a variable X ; X is any value of the variable from X_{min} to X_{max} ; X_{min} is the lower limit of the variable and X_{max} is the upper limit of the variable. The chosen levels of the selected process parameters with their units and notations are given in Table 2.

The design matrix chosen to conduct the experiments was a central composite rotatable design (Ref. 11), which is shown in Table 3. In this work, 31 deposits were made using a cladding condition corresponding to each treatment combination of parameters as shown in Table 3 at random. At the end of each run, settings for all four parameters were disturbed and reset for the next deposit. This was essential to introduce variability caused by errors in experimental settings (Ref. 12).

A typical clad plate is shown in Fig. 2. To measure the FN of the clad metals, the clad plates were cross sectioned at their midpoints to obtain test specimens of 20 mm wide. The top surface of each specimen was ground flat. The FN measurement was carried out using a Ferritescope. Six readings were taken on the top surface along the longitudinal axis of the three beads with the Ferritescope calibrated in accordance with procedures specified in ANSI/AWS A4.2. The average values found are given in Table 3. Using the same specimens, three test burns were taken on the top surface of the claddings to find out chemical composition using an optical emission spectrometer (ARL 3460). The average of three readings was calculated and tabulated in Table 4. Figure 3 shows the locations of the FN and chemical analysis measurements. The chromium and nickel equivalents (Cr_{eq} and Ni_{eq}) of WRC-1992 Diagram were calculated using Equations 2 and 3. These values are also given in Table 4.

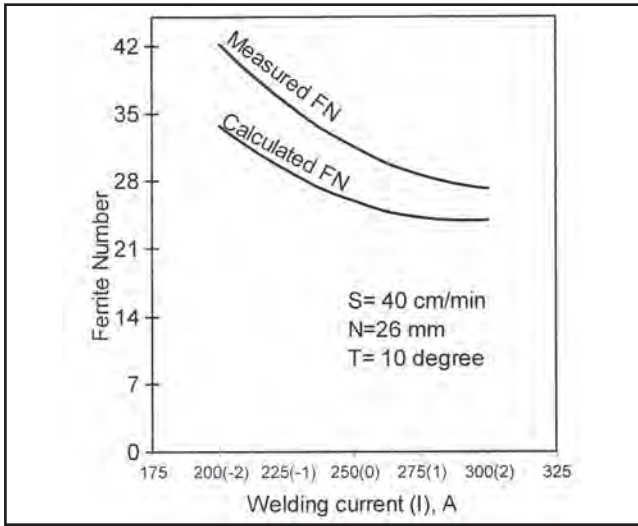


Fig. 7 — Effect of welding current on calculated and measured FN.

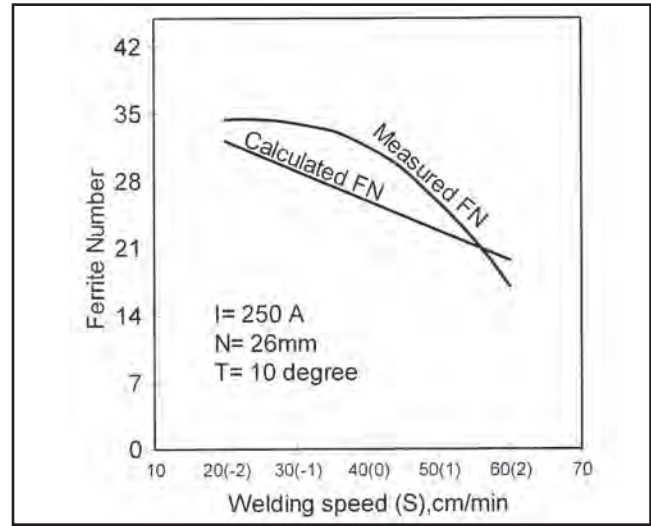


Fig. 8 — Effect of welding speed on calculated and measured FN.

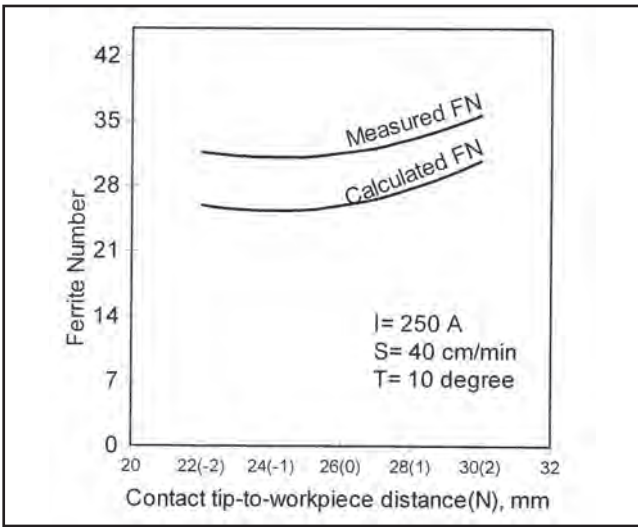


Fig. 9 — Effect of contact tip-to-workpiece distance on calculated and measured FN.

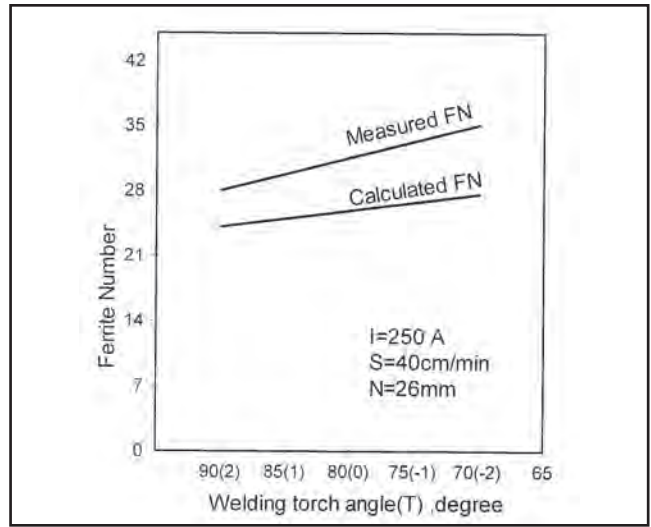


Fig. 10 — Effect of welding gun angle on calculated and measured FN.

$$Cr_{eq} = Cr + Mo + 0.7Nb \quad (2)$$

$$Ni_{eq} = Ni + 35C + 20N + 0.25Cu \quad (3)$$

From the calculated chromium and nickel equivalents, FN values were predicted using WRC-1992 Constitution Diagram in Table 3. To study the effect of process parameters on dilution, dilution values for all specimens were measured using the following procedure. Each weld was cross sectioned at mid length, polished and etched with 2% Nital. The bead profiles were traced using a reflective type optical profile projector at a magnification of 10X, and then the deposit area and plate fusion area were measured using a digital planimeter. The measured dilution values are given in Table 3.

Development of Mathematical Models

The response function representing FN can be expressed using the equation

$$Y = f(X_1, X_2, X_3, X_4) \quad (4)$$

where Y = response [FN], X_1 = welding current (I) in A, X_2 = welding speed (S) in cm/min, X_3 = contact tip-to-workpiece distance (N) in mm, and X_4 = welding gun angle (T) in degrees.

The second order response surface model (Ref. 13) for the four selected parameters is given by Equation 5.

$$Y = \beta_0 + \sum_{i=1}^4 \beta_i X_i + \sum_{i=1}^4 \beta_{ii} X_i^2 + \sum_{i=1}^4 \sum_{j=1}^4 \beta_{ij} X_i X_j \quad (5)$$

The above second order response surface model could be expressed as follows:

$$Y = \beta_0 + \beta_1 I + \beta_2 S + \beta_3 N + \beta_4 T + \beta_{11} I^2 + \beta_{22} S^2 + \beta_{33} N^2 + \beta_{44} T^2 + \beta_{12} IS + \beta_{13} IN + \beta_{14} IT + \beta_{23} SN + \beta_{24} ST + \beta_{34} NT \quad (5A)$$

Where β_0 is free term of the regression equation, the coefficients $\beta_1, \beta_2, \beta_3,$ and β_4 are linear terms, the coefficients $\beta_{11}, \beta_{22},$

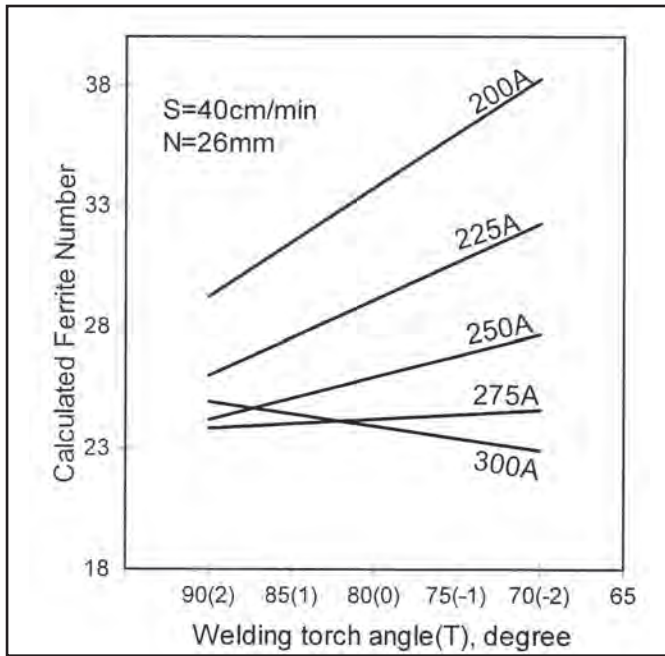


Fig. 11 — Interaction effects of welding current and welding gun angle on calculated FN.

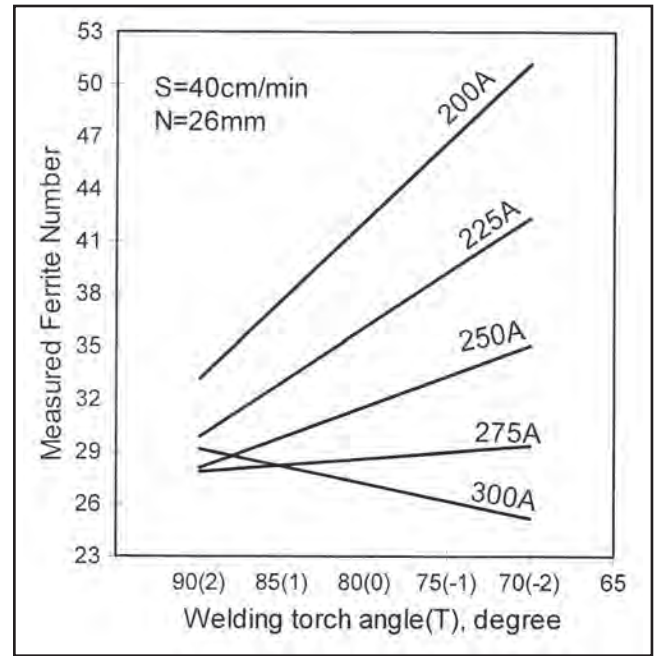


Fig. 12 — Interaction effects of welding current and welding gun angle on measured FN.

Table 4 — Cladding Compositions

Trial No.	Elements, %										Equivalents	
	Cr	Mo	Nb	Ni	C	N	Cu	Mn	Si	Cr _{eq}	Ni _{eq}	
1	21.64	3.05	0.018	8.86	0.037	0.132	0.058	0.902	0.598	24.71	12.81	
2	21.10	3.08	0.018	8.56	0.041	0.140	0.056	0.903	0.575	24.20	12.80	
3	21.24	3.06	0.018	8.76	0.035	0.137	0.055	0.925	0.633	24.31	12.74	
4	19.96	2.87	0.017	8.08	0.053	0.119	0.052	0.930	0.598	22.85	12.32	
5	21.88	3.20	0.018	9.32	0.036	0.134	0.056	0.892	0.581	25.09	13.08	
6	21.22	3.00	0.017	8.38	0.037	0.134	0.053	0.9916	0.570	24.23	12.85	
7	21.28	3.13	0.018	8.73	0.038	0.155	0.056	0.959	0.651	24.43	13.17	
8	20.50	2.80	0.017	8.00	0.041	0.138	0.054	0.937	0.602	23.32	12.21	
9	21.59	3.02	0.018	8.99	0.029	0.142	0.057	0.928	0.590	24.63	12.86	
10	20.78	3.03	0.017	8.41	0.041	0.113	0.052	0.839	0.537	23.82	12.12	
11	19.16	2.86	0.017	7.74	0.053	0.107	0.049	0.899	0.557	22.03	11.73	
12	19.02	2.73	0.017	7.70	0.052	0.110	0.049	0.900	0.555	21.76	11.74	
13	21.85	3.10	0.019	9.08	0.029	0.141	0.059	0.919	0.626	24.96	12.73	
14	21.03	3.16	0.018	8.67	0.039	0.134	0.056	0.936	0.583	24.20	12.73	
15	20.21	2.94	0.017	7.85	0.047	0.104	0.051	0.934	0.571	23.17	11.59	
16	19.21	2.71	0.017	8.24	0.047	0.117	0.050	0.858	0.527	21.92	12.23	
17	21.94	3.28	0.019	8.34	0.031	0.131	0.060	0.978	0.676	25.23	12.75	
18	19.98	2.98	0.017	7.61	0.053	0.132	0.052	0.912	0.568	22.97	12.66	
19	21.48	3.27	0.018	8.85	0.030	0.144	0.057	0.866	0.545	24.76	12.78	
20	19.27	2.80	0.016	7.46	0.043	0.156	0.048	0.934	0.579	22.07	12.48	
21	20.54	2.91	0.017	8.40	0.041	0.116	0.052	0.939	0.636	21.02	12.17	
22	21.37	3.15	0.018	8.71	0.036	0.117	0.053	0.901	0.542	24.53	12.32	
23	20.31	2.99	0.017	8.31	0.045	0.119	0.053	0.917	0.559	23.31	12.29	
24	19.81	2.90	0.017	8.09	0.050	0.112	0.053	0.909	0.560	22.72	12.09	
25	20.76	2.98	0.018	8.63	0.033	0.124	0.055	0.914	0.603	23.75	12.28	
26	21.04	2.95	0.018	8.08	0.055	0.139	0.050	0.890	0.534	23.70	12.80	
27	21.05	3.11	0.018	8.63	0.033	0.124	0.055	0.982	0.642	24.17	12.28	
28	20.61	3.12	0.018	8.44	0.041	0.114	0.053	0.916	0.608	23.74	12.17	
29	20.43	2.95	0.018	8.63	0.033	0.124	0.055	0.928	0.619	23.40	12.25	
30	20.13	2.95	0.018	8.27	0.034	0.123	0.052	0.935	0.610	23.10	11.94	
31	20.18	2.95	0.018	8.63	0.033	0.124	0.055	0.942	0.598	23.14	12.28	

β_{33} , and β_{44} are quadratic terms, and the coefficients β_{12} , β_{13} , β_{14} , β_{23} , β_{24} , and β_{34} are interaction terms. The coefficients were calculated using QA six sigma software

and the same was verified by using SYS-TAT 10.2 software. After determining the coefficients, the mathematical models (Equations 6 and 7) were developed as

follows:

$$\begin{aligned} \text{Calculated FN (By WRC-1992 Diagram)} \\ = 26.429 - 2.458I - 3.125S + 1.208N \\ - 0.875T + 0.674I^2 - 0.076S^2 + 0.549N^2 \end{aligned}$$

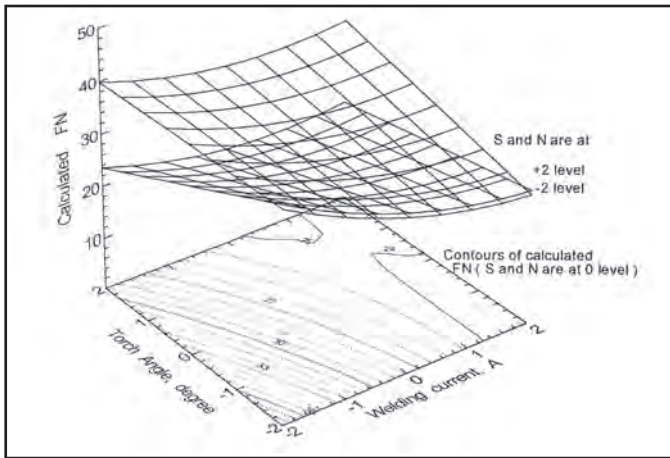


Fig. 13 — Contour plot and response surface plot for interaction effects of welding current and welding gun angle on calculated FN.

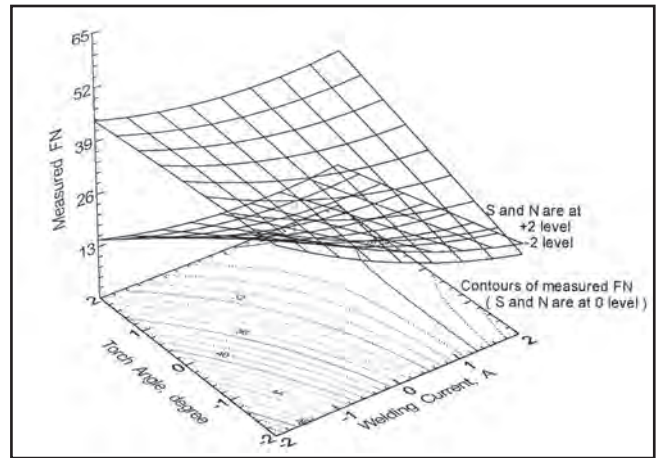


Fig. 14 — Contour plot and response surface plot for interaction effects of welding current and welding gun angle on measured FN.

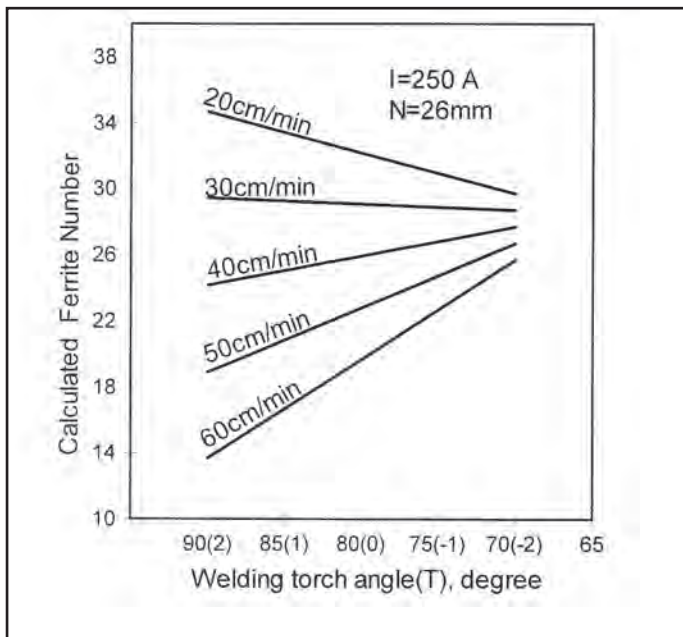


Fig. 15 — Interaction effects of welding speed and welding gun angle on calculated FN.

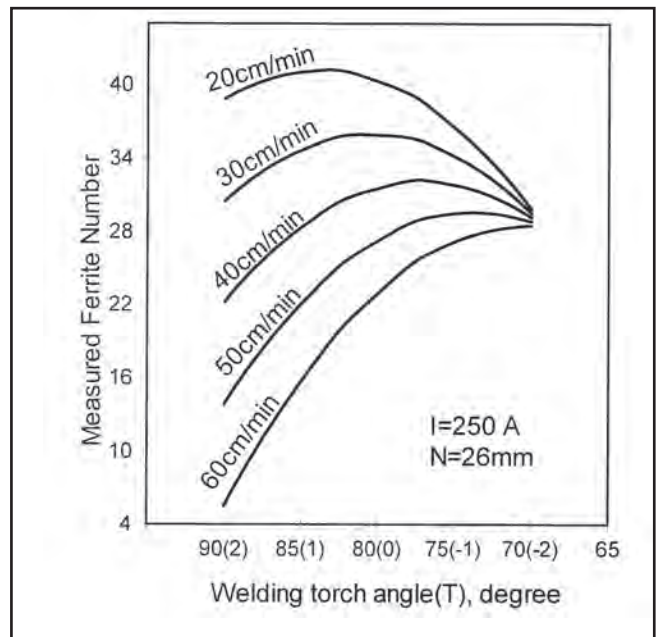


Fig. 16 — Interaction effects of welding speed and welding gun angle on measured FN.

$$- 0.451T^2 - 0.562S - 0.188IN + 0.688IT + 0.312SN - 1.062ST + 0.562NT \quad (6)$$

$$\begin{aligned} \text{Measured FN} = & 32.000 - 3.750I - 4.333S \\ & + 1.000N - 1.750T + 0.729I^2 - 1.521S^2 \\ & + 0.479N^2 - 0.396T^2 - 0.375IS - 0.375IN \\ & + 1.375IT + 0.250SN - 2.000ST + 0.250NT \quad (7) \end{aligned}$$

To develop final mathematical models, the insignificant coefficients were eliminated without affecting the accuracy of the developed models by using t-test. This is done by back elimination technique, using QA six sigma software and the same was verified by using SYSTAT 10.2 software.

The final mathematical models were constructed by using these coefficients. The developed final mathematical models (Equations 8 and 9) with process param-

eters in coded form are given below.

$$\begin{aligned} \text{Calculated FN (By WRC-1992 Diagram)} \\ = & 25.942 - 2.458I - 3.125S + 1.208N \\ & - 0.875T + 0.725I^2 + 0.600N^2 + 0.688IT \\ & - 1.062ST \quad (8) \end{aligned}$$

$$\begin{aligned} \text{Measured FN} = & 31.596 - 3.750I - 4.333S \\ & + 1.000N - 1.750T + 0.771I^2 - 1.479S^2 \\ & + 0.521N^2 + 1.375IT - 2.000ST \quad (9) \end{aligned}$$

It was found that the reduced models are better than the full models because the reduced models have higher values of R^2 (adjusted) and lesser values of standard error of estimates than that of full models. The values of R^2 (adjusted) and standard error of estimates for full and reduced models are given in Table 6.

The adequacies of the developed models were tested using the analysis of variance (ANOVA) technique (Ref. 14). As per this technique, if the calculated F-ratio values for the developed models do not exceed the standard tabulated values of F-ratio for a desired level of confidence (95%), and the calculated R-ratio values of the developed models exceed the standard tabulated values of R-ratio for a desired level of confidence (95%), then the models are said to be adequate within the confidence limit. The calculated values of F-ratio and R-ratio are given in Table 7. This shows that the developed models are adequate. The validity of these models were again tested by drawing scatter diagrams as shown in Fig. 4A and B, which show the observed and predicted values of

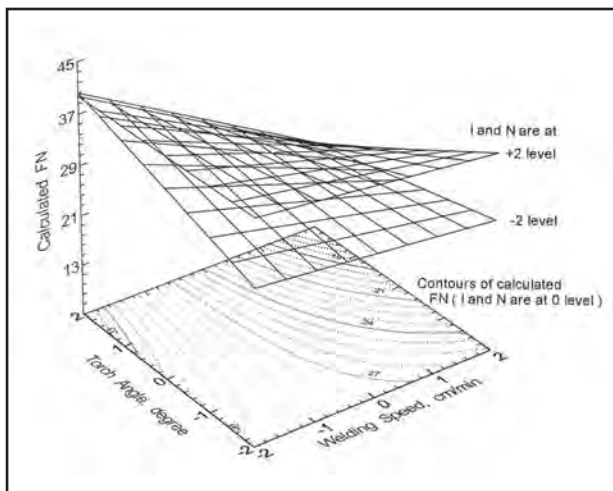


Fig. 17 — Contour plot and response surface plot for interaction effects of welding speed and welding gun angle on calculated FN.

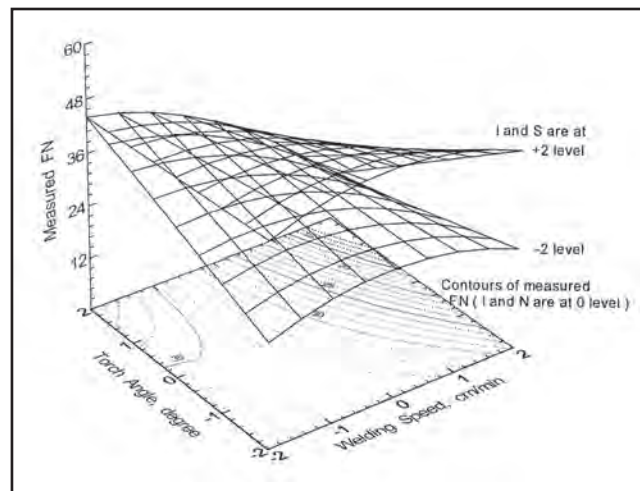


Fig. 18 — Contour plot and response surface plot for interaction effects of welding speed and welding gun angle on measured FN.

Table 5 — Heat Input and Corresponding Values of Dilution and FN

S. No.	Trial No.	I	S	N	T	V (Volts)	Heat Input (kJ/mm)	Dilution (%)	Calculated FN	Measured FN
1	17	200	40	26	80	32	0.96	05.86	34	47
2	07	225	50	28	75	38	1.00	09.69	29	37
3	28	250	40	26	80	40	1.50	11.71	28	33
4	02	275	30	30	75	43	2.37	12.10	27	31

calculated and measured FN.

Conformity tests were conducted using the same experimental setup to conform the results of the experiments. The results of the conformity tests shown in Table 8 depict the accuracy of the developed models, which is above 94%.

Results and Discussions

The above developed models (Equations 8 and 9) can be used to predict the calculated FN (by WRC-1992 Diagram) and the measured FN by substituting the coded values (-2, -1, 0, +1, +2) of the respective process parameters. The effects of heat input and dilution on FN are represented in graphical form in Figs. 5 and 6. The responses calculated using the developed mathematical models for each set of coded welding parameters are also represented in graphical form in Figs. 7-18.

Effects of Heat Input on FN

Heat input is a relative measure of the energy transferred per unit length of weld. It is an important characteristic because it influences the cooling rate, which may affect the mechanical properties and metallurgical structure of the weld and heat-affected zones. Heat input is typically cal-

culated as the ratio of the power (i.e., voltage x current) to the velocity of the heat source (i.e., the arc). In this study, the heat input values were calculated for specimens welded at cladding conditions corresponding to trial numbers 2, 7, 17, and 28, which are given in Table 5. These are represented in graphical form in Fig. 5. It is evident from Fig. 5 that the FN increases with a decrease in heat input. At higher cooling rates (low heat input), the transformation of ferrite to austenite will be suppressed, resulting in higher residual ferrite content in the claddings (Refs. 15 and 16).

Effects of Dilution on FN

The composition and properties of clad metals are strongly influenced by the dilution obtained. Control of dilution is very important in cladding, where low dilution is typically desirable. When the dilution is low, the final deposit composition is close to that of the filler metal, and the corrosion resistance of the cladding is maintained.

The calculated values of dilution for trial numbers 2, 7, 17, and 28 (Table 5) are represented in graphical form in Fig. 6. It is evident from Fig. 6 that FN decreases with increases in dilution. An increase in dilution enhances the C content and reduces the Cr and Ni content of the

cladding. The reduction of Cr and Ni and the enhancement of C in the cladding with the increase of dilution occurred primarily because the base metal had no Cr and Ni and higher C with respect to the chemical composition of the duplex stainless steel electrode.

The change in dilution governing chemical composition of the cladding affects chromium and nickel equivalents (Ref. 17) estimated by the WRC-1992 Diagram. The increase in dilution reduces chromium equivalent and moderately decreases the nickel equivalent of the cladding, which results in reduced FN. The lower dilution in claddings resulted in higher FN in the clad metals (Ref. 18).

Direct Effects of Process Parameters on Calculated and Measured FN

Direct Effects of Welding Current on Calculated and Measured FN

From Fig. 7 it is evident that calculated and measured FN decrease with an increase in welding current. This may be due to an increase in heat input and dilution with an increase in welding current. An increase in welding current resulting in enhanced heat input and higher current density causing a larger volume of the base plate to melt and hence increased dilution. This decreases the FN of the claddings.

Direct Effects of Welding Speed on Calculated and Measured FN

From Fig. 8 it is evident that the calculated and measured FN decrease with an increase in welding speed. This may be due to increased dilution of the base metal in the pool with an increase in welding speed, since the weight of deposited metal per unit of length decreases while the

cross section of the bead decreases very little (Refs. 19 and 20). The speed, therefore, exerts an influence on the composition of the weld bead analogous to that of current. The effect of dilution is more dominant than the effects of heat input on the FN with increased welding speed, hence the FN decreases with the increase in welding speed.

Direct Effects of Contact Tip-to-Workpiece Distance on Calculated and Measured FN

It is evident from Fig. 9 that calculated and measured FN increase slightly with an increase in contact tip-to-workpiece distance. An increase in contact tip-to-workpiece distance increases the circuit resistance, which reduces the welding current. This decrease of welding current reduces the penetration of the arc, and hence, reduces the dilution (Ref. 21). The decrease in dilution increases the FN of the clad metals. The changes in contact tip-to-workpiece distance do not affect the heat input much.

Direct Effects of Welding Gun Angle on Calculated and Measured FN

From Fig. 10 it is evident that calculated and measured FN increase with the increase in welding gun angle. The reason is when the angle is increased in forehand welding, the arc force pushes the weld metal forward, i.e., toward the cold metal, which reduces penetration and dilution (Ref. 22). This results in increased FN of the clad metals. The changes in welding gun angle do not affect the heat input much.

Interaction Effects of Process Parameters on Calculated and Measured FN

Interaction Effects of Welding Current and Welding Gun Angle on Calculated and Measured FN

From Figs. 11 and 12 it is evident that the FN decreases with an increase in welding gun angle when welding current is from 200 to 275 A, and the rate of increase in FN also decreases with an increase in welding current up to 275 A. But when welding current is 300 A, the FN decreases with a decrease in welding gun angle. Figures 13 and 14 show the response surface and the contour plot of FN for the interaction of welding gun angle and welding current. From the contour surface, it is found that the FN has its lowest value when welding current is at its maximum value and the welding gun angle is at its maximum value. The highest value of FN is obtained when welding current is at its minimum value and the welding gun angle is at its minimum value.

Interaction Effects of Welding Speed and Welding Gun Angle on Calculated and Measured FN

From Figs. 15 and 16 it is evident that

FN increases with a decrease in welding gun angle when welding speed is from 40 to 60 cm/min. The rate of increase in FN also decreases with the increase in welding speed up to 40 cm/min, but when welding speed is from 20 to 40cm/min, FN decreases with a decrease in welding gun angle. Figures 17 and 18 show the response surface and the contour plot of FN for interaction of welding gun angle and welding speed. From the contour surface, it is found that the FN has the lowest value, when welding speed is at its maximum value and the welding gun angle is at its maximum value. The FN has highest value when welding speed is at its minimum and the welding gun angle is at its maximum value.

Conclusions

The effects of welding current, welding speed, contact tip-to-workpiece distance, and welding gun angle on the FN in duplex stainless steel deposits were investigated. The following are the conclusions derived from this investigation:

- 1) A five-level, four-factor full-factorial design matrix based on the central composite rotatable design technique can be used for the development of mathematical models to predict calculated (by WRC-1992

Table 6 — Comparison of R² Values and Standard Error of Estimates for Full and Reduced Models

Parameters	R ² values		Standard error of estimates	
	Full models	Reduced models	Full models	Reduced models
Calculated FN	0.757	0.780	2.160	2.053
Measured FN	0.833	0.863	2.529	2.290

Table 7 — Analysis of Variance for Testing Adequacy of the Models

Parameter	1st order Terms		2nd order Terms		Lack of fit		Error terms		F-ratio	R-ratio	Whether model is adequate
	SS	DF	SS	DF	SS	DF	SS	DF			
FN(C)	433	4	67	10	36.92	10	37.8	6	0.547	9.590	adequate
FN (M)	852	4	194	10	91.00	10	12.0	6	3.406	59.82	adequate

FN(C) – Calculated FN, FN (M) – Measured FN, SS – Sum of squares, DF – Degrees of freedom
 F-ratio (10, 6, 0.05) = 4.09, R-ratio (14, 6, 0.05) = 3.96

Table 8 — Results of Conformity Tests

I	Process parameter in Coded form			Predicted Values of FN (using models)		Actual Values of FN		Error, %	
	S	N	T	FN(C)	FN (M)	FN(C)	FN (M)	FN (C)	FN (M)
-0.11	-0.22	0.09	-0.3	27	33	28	32	3.70	-3.03
-0.79	-0.35	0.94	1.02	30	36	30	34	0.00	-5.56
-0.66	0.03	0.90	1.03	28	39	28	40	0.00	2.56

% Error = $\frac{\text{Actual value} - \text{Predicted value}}{\text{Predicted value}} \times 100$. FN(C) – Calculated FN, FN (M) – Measured FN

Diagram) and measured FN of duplex stainless steel cladding deposited by FCAW.

2) The Ferrite Number calculated from the cladding compositions using WRC-1992 Diagram agrees reasonably well with the measured FN.

3) The Ferrite Number decreases with the rise in heat input and dilution.

4) The Ferrite Number decreases with a rise in welding current and welding speed and increases with a decrease in welding gun angle and rise in contact tip-to-work-piece distance.

5) A decrease in welding gun angle increases the FN when welding current was low, but the FN decreases slightly with a decrease in welding gun angle when welding current was high.

6) A decrease in welding gun angle increased the FN when welding speed was high, but the FN decreased slightly with a decrease in welding gun angle when welding speed was low.

Acknowledgments

The authors wish to thank M/S Bohler welding, Austria, for providing flux cored duplex stainless steel welding wire for this work. The financial support for this work from All India Council of Technical Education and University Grants Commission are gratefully acknowledged. The authors also wish to thank the management of Coimbatore Institute of Technology and Kumaraguru College of Technology for providing all the necessary facilities to carry out this research work.

References

- Hasson, D. F., Zanis, C., Aprigliano, L., and Fraser. 1978. Surfacing of 3.25% nickel steel with Inconel® 625 by the gas metal arc welding-pulsed arc process. *Welding Journal* 57(1): 1-s to 8-s.
- Karlsson, L., Ryen, L., and Pak, S. 1995. Precipitation of intermetallic phases in 22% duplex stainless steel weld metals. *Welding Journal* 74(1): 28-s to 40-s.
- Kotecki, D. J. 1997. Ferrite determination in stainless steel welds. *Welding Journal* 76(1): 24-s to 36-s.
- Siewert, T. A., McCowan, C. N., and Olson, D. L. 1988. Ferrite Number prediction to 100FN in stainless steel weld metal. *Welding Journal* 67(12): 289-s to 298-s.
- Welding, brazing, and soldering. 1993. *ASM Handbook*, Volume 6, ASM International, Materials Park, Ohio.
- Schaeffler, A. L. 1949. Constitution diagram for stainless steel welds metal. *Metal Progress* 56(11): 680 to 680B.
- Kotecki, D. J. 1978. Welding parameters effects on open-arc stainless steel weld metal ferrite. *Welding Journal* 57(4): 109-s to 117-s.
- DeLong, W. T. 1974. Ferrite in austenitic stainless steel weld metal. *Welding Journal* 53(7): 273-s to 286-s.
- Kotecki, D. J., and Siewert, T. A. 1992. WRC-1992 Constitution diagram for stainless steel weld metals: A modification of the WRC-1988 Diagram. *Welding Journal* 57(4): 171-s to 178-s.
- Murugan, N., and Parmer, S. 1995. Effects of MIG process parameters on the geometry of the bead in the automatic surfacing of stainless steel. *International Journal for the Joining of Materials* 7(2): 71 to 80.
- Cochran, W. G., and Cox, G. M. 1987. *Experimental Designs*. p. 370, New York, John Wiley & Sons.

12. Harris, P., and Smith, B. L. 1983. Factorial technique for weld quality prediction. *Metal Construction* 15(11): 661 to 666.

13. Montgomery, D. C. 2003. *Design and Analysis of Experiments*. p. 429. John Wiley & Sons (ASIA) Pte. Ltd.

14. Gunaraj, V., and Murugan, N. 1999. Prediction and comparison of the area of the heat-affected zone for the bead on plate and bead on joint in submerged arc welding of pipes. *Journal of Material Processing Technology* 95: 246 to 261.

15. Vitek, J. M., David, S. A., and Hinman, C. R. 2003. Improved ferrite number prediction model that accounts for cooling rate effects — part 1: model development. *Welding Journal* 82(1): 10-s to 17-s.

16. Vitek, J. M., David, S. A., and Hinman, C. R. 2003. Improved ferrite number prediction model that accounts for cooling rate effects — part 2: model results. *Welding Journal* 82(2): 43-s to 50-s.

17. Ghosh, P. K., Gupta, P. C., and Goyal, V. K. 1998. Stainless steel cladding of structural steel plate using the pulsed current GMAW process. *Welding Journal* 77(7): 307-s to 314-s.

18. Kotecki, D. J. 1996. Dilution control in single wire stainless steel submerged arc cladding. *Welding Journal* 75(2): 35-s to 45-s.

19. Jean Cornu. 1988. *Advanced Welding Systems*, Vol. 2, IFS (Publications) Ltd., U.K.

20. Raveendra, J., and Parmar, R. S. 1987. Mathematical models to predict weld bead geometry for flux cored arc welding. *Metal Construction* 189(1): 31R to 35R.

21. Kim, J. W., and Na S. J. 1995. A study on the effect of contact tube-to-workpiece distance on weld pool shape in gas metal arc welding. *Welding Journal* 74(5): 141-s to 152-s.

22. Funk and Rieber. 1985. *Handbook of Welding*, PWS-KENT Publishing Co.

CAN WE TALK?

The *Welding Journal* staff encourages an exchange of ideas with you, our readers. If you'd like to ask a question, share an idea or voice an opinion, you can call, write, e-mail or fax. Staff e-mail addresses are listed below, along with a guide to help you interact with the right person.

Publisher/Editor

Andrew Cullison
cullison@aws.org, Extension 249
 Article Submissions

Senior Editor

Mary Ruth Johnsen
mjohnsen@aws.org, Extension 238
 Feature Articles

Associate Editor

Howard Woodward
woodward@aws.org, Extension 244
 Society News
 Personnel

Assistant Editor

Kristin Campbell
kcampbell@aws.org, Extension 257
 New Products
 News of the Industry

Managing Editor

Zaida Chavez
zaida@aws.org, Extension 265
 Design and Production

Advertising Sales Director

Rob Saltzstein
salty@aws.org, Extension 243
 Advertising Sales

Advertising Sales & Promotion Coordinator

Lea Garrigan
garrigan@aws.org, Extension 220
 Production and Promotion

Advertising Production Manager

Frank Wilson
fwilson@aws.org, Extension 465
 Advertising Production

Peer Review Coordinator

Erin Adams
eadams@aws.org, Extension 275
 Peer Review of Research Papers

Welding Journal Dept.
 550 N.W. LeJeune Rd.
 Miami, FL 33126
 (800) 443-9353
 FAX (305) 443-7404